

Special Issue: Energy in Agriculture

Scientific Paper

Doi: <http://dx.doi.org/10.1590/1809-4430-Eng.Agric.v42nepe20220108/2022>

ELECTRICAL PERFORMANCE OF A WATER-COOLED PVT SYSTEM WITH FORCED AND NATURAL CIRCULATION

**Bruno M. Antunes^{1*}, Rodrigo A. Jordan¹, Anamari V. de A. Motomiya¹,
Rodrigo C. Santos¹, Orlando Moreira Júnior¹**

^{1*}Corresponding author. Universidade Federal da Grande Dourados - UFGD/Dourados - MS, Brasil.

E-mail: brunomachadoantunes@hotmail.com | ORCID ID: <https://orcid.org/orcid.org/0000-0002-4222-0787>

KEYWORDS

Boiler, photovoltaic-thermal panel, thermal accumulation.

ABSTRACT

This study evaluated the electrical performance of a photovoltaic-thermal (PVT) system using water as a cooling fluid (PVT/w), with adaptation, in a photovoltaic module of a device for heating water without direct contact with the cell and with air as the secondary working fluid. The PVT/w system with forced and natural circulation was compared in a regime of thermal accumulation of hot water and supply by a boiler reservoir relative to the same PV panel with the original factory characteristics. The average system temperature, open circuit voltage, current and voltage with load, and generated electric power were analyzed during seven non-consecutive days, with ten repetitions every thirty minutes between 9:30 am and 2:00 pm in the city of Dourados-MS, Brazil, between June and July 2021. The PVT system with forced circulation (PVT/w_CB) presented the best electrical performance compared to the PVT system with natural circulation (PVT/w_SB), in the order of 3.7%.

INTRODUCTION

Demand for food and energy is estimated to be 50% higher by 2050 than it was in 2017 due to population growth approaching 10 billion people (UN, 2022). Thus, the use of energy systems from renewable sources is a favorable way to meet this energy demand, especially solar and wind, easily used in rural areas (Rahman et al. 2022).

According to Queiroz & Brito (2020), solar energy for small-and medium-sized agro-industry has received large financial contributions and a focus on research, as the efficiency of systems can be greatly improved.

The production of electrical energy through the photovoltaic effect stands out in the use of solar energy, whose conversion is carried out by the panel or photovoltaic (PV) module. According to Cotfas et al. (2022), nominal operating temperature is one of the main factors that influence its efficiency due to the electrical properties of semiconductors and other components. The output voltage drops, and a small variation of the current values is observed as the temperature increases, which causes a decrease in the power of the module.

The literature commonly presents some coefficients to represent the effect of temperature on the electrical characteristics of the modules, being normally indicated negatively in percentage per temperature unit, such as coefficient of variation of the short-circuit current (α), coefficient of variation of the open-circuit voltage (β) coefficient of variation of the and maximum power (γ) (Tarbi et al., 2022; Ouédraogo et al., 2021).

A hybrid photovoltaic/thermal (PVT) system combines a photovoltaic module and a solar thermal collector (T), simultaneously producing electrical and thermal energy in the same equipment (Hajjaj et al., 2019). The idea of this equipment is to take advantage of the waste heat from the electrical energy generation of the panel to heat some fluid, increasing the amount of energy per square meter, but with increasing the electrical efficiency of the panel being its main objective (Tiwari et al., 2018). This concept is not recent, as the subject has been researched since the end of the 1970s (Kern Jr & Russell, 1978).

¹Universidade Federal da Grande Dourados - UFGD/Dourados - MS, Brasil.

Area Editor: Juliana Lobo Paes

Received in: 6-30-2022

Accepted in: 8-25-2022

PVT systems can be classified according to their constructive aspect (presence or absence of a glass cover), refrigerant fluid (liquid or gaseous), fluid transportation (natural or forced), photovoltaic module technology (monocrystalline, polycrystalline, amorphous, etc.), and type of collector (flat plate or concentrator type), among other structural characteristics (Lammle et al., 2017).

According to Hossain et al. (2019), PVT systems with a glass cover have higher thermal efficiency in exchange for lower electrical efficiency, as the amount of heat lost to the environment is reduced but will have a higher reflection of the sun rays. On the other hand, PVT systems without a glass cover, which are typically commercial models, result in lower thermal efficiency and higher electrical efficiency.

Hassan et al. (2020) states that the PVT system using air as a refrigerant fluid (PVT/a), naturally or forced, provides a simple and economical solution to cool the modules, with the forced form presenting the best heat transfer ratio, but at the cost of a smaller share of net electricity. A PVT/w system uses water as a thermal fluid in the cooling of the photovoltaic system. Regarding heat removal, these systems are more efficient than PVT/a systems due to the higher thermal conductivity of water compared to air (Ahmed et al., 2019).

Given the different constructive characteristics that thermal systems used in agriculture can present in their composition and their direct influence on the resulting final efficiency, this study aimed to analyze the electrical performance of a PV system adapted to operate as PVT/w, operating with natural and forced circulation, and comparing operational parameters.

MATERIAL AND METHODS

The tests were carried out in an experimental field area located at the School of Agricultural Sciences (FCA) of the Federal University of Grande Dourados (UFGD), in Dourados, Mato Grosso do Sul, Brazil, at the geographic coordinates 22°11'53" S and 54°56'03" W and an average altitude of 408 m. The region is characterized by a tropical climate, with an average annual temperature of 26 °C and annual accumulated rainfall of 1,110 mm. The climate is Aw,

according to the Köppen classification (Alvares et al., 2013). The experiment was carried out from June to July 2021.

The chosen PVT/w system was a variation of the shell-and-tube model, assembled from the adaptation of the coil of a solar water heating collector inside a photovoltaic panel. The proposed PVT/w system had no direct contact of the coil (heat exchanger) with the cells of the photovoltaic panel. Thus, the heat transfer mechanism between the cells and the heat exchanger was by convection, using the air trapped in the enclosure as a secondary fluid.

The coil (Figures 1 and 2) was taken from a CSVM-BV 200 solar water heating collector, with dimensions of 1,976×1,016 mm, a weight of 27.2 kg, and a nominal working pressure of 40 mWC.

The photovoltaic module consisted of a YINGLI SOLAR YL140P-17b composed of 36 polycrystalline cells, with dimensions of 1,470×680 mm, maximum power (Pmax) of 140 W, electrical efficiency of 14%, maximum power voltage (Vmp) of 18.01 V, and maximum power current (Imp) of 7.77 A.

The system had an exchanger with five 6-mm copper tubes, surrounded by a folded aluminum plate, connected to a 22-mm collector tube at one end (Figure 1a) welded to a second collector tube, also 22 mm long, coming from the cut of the solar collector coil. One end of each collector tube was left outside the panel for the water circulation connections. The opposing limits, which were inside the panel, were closed with bending and welding. Thus, the PVT/w had only one water inlet and one water outlet on one of its sides (Figure 1c).

The back of the photovoltaic panel was closed with an 11-mm thick plasticized plywood board after installing the heat exchanger, aiming to minimize heat losses at the rear of the equipment and allow heat exchange to occur between the water and the air trapped in the created enclosure.

The PVT/w system is designed to operate in a closed environment, in which there is recirculation of water without replenishment. The choice of this type of system was due to the objective of storing heat for use. Thus, the PVT/w system was connected to a boiler with a volumetric capacity of 250 liters. Natural circulation by thermosiphon and forced circulation by employing a 35 W electric pump (220 V) with a volumetric flow of 14 L min⁻¹ were used.



FIGURE 1. (a) Front and (b) rear views of the heat exchanger module and (c) heat exchanger adapted inside the photovoltaic panel.



FIGURE 2. (a) Front and (b) rear views of the assembled PVT/w system.

Water was supplied in the PVT/w system through the lower end of the collector tube, with the outlet through the upper end, both with installed temperature sensors. The electric pump was installed between the water outlet of the PVT/w system and the boiler, which was installed on a base 90 cm high from the ground. A 25-mm diameter PVC pipe

was used to connect the PVT/w system equipment.

Another board identical to the one used in the PVT/w system but without any change (PV) was used for comparison. Both panels were installed in an open environment, one next to the other, sloping at 26° and oriented to the geographic north (Figure 3).

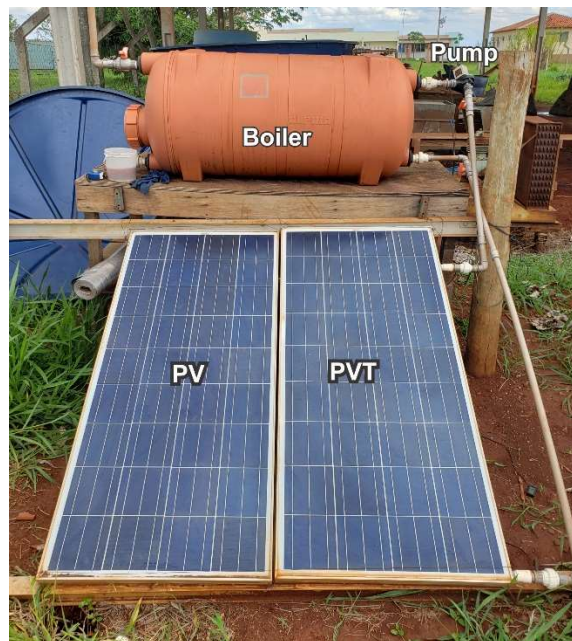


FIGURE 3. View of the PV and PVT system installation and boiler.

A fixed load electrical resistor bank (without variation) was used to simulate loads and obtain the electrical parameters of the panels. The arrangement was composed of three 10 Ω resistors associated in parallel. This association resulted in an equivalent resistance equal to 3.33 Ω .

As the panel STC conditions are ideal and, therefore, obtained only in the laboratory, the used resistor bank was also dimensioned considering that the system would operate with 85% of the maximum power informed by the nominal operating cell temperature (NOCT) method, which

considers a more severe condition, that is, more realistic. In addition, the panel cannot provide maximum power all the time, as the radiation varies throughout the day.

Figure 4 shows the electrical arrangement of the resistor bank, the way the measuring instruments were positioned, and the mounted resistor bank.

The following parameters were measured during the tests: surface temperature of the panels, open-circuit voltage, voltage with load, and electric current.

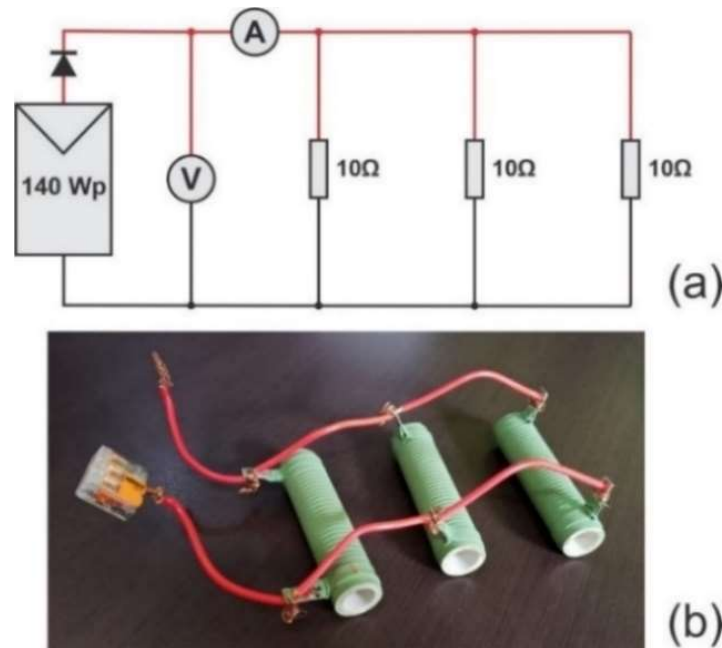


FIGURE 4. (a) Diagram of the load bank and (b) resistor bank.

The electric pump was turned on for a few minutes at the end of each test until the internal temperatures of the boiler were homogenized in the tests with natural circulation, thus avoiding possible water temperature gradients due to the difference in density. Failure to carry out this procedure could lead to a false reading of the value taken as being representative of the average temperature value of the water inside the boiler since its sensor was located in the medium.

The meteorological data were obtained from the UFGD automatic weather station, located at coordinates 22°11'35.4" S and 54°55'35.0" W, whose distance in a straight line to the experiment site was approximately 967 m.

An M890C+ digital multimeter with an accuracy of $\pm 0.5\%$ in the direct current voltage (DCV) function was used for measurements of electrical parameters.

Temperature measurements on the surface of the panels were performed with a GM420 digital infrared pyrometer with a precision of ≤ 0.5 °C and measurement ranges from -50 to 420 °C. The average temperature was determined considering the arithmetic mean of three different points on their surfaces (bottom, center, and top).

Two digital sensors with an LCD, precision of ± 1.0 °C, and range from -50 to 110 °C were used for the water inlet and outlet temperatures in the panels. An NTC probe sensor, connected to a Coel TLZ-10 temperature controller, used as a reading indicator, was employed for the temperature measurement inside the boiler.

Analyzed variables

The average temperature of the panels was determined considering the arithmetic mean of three different points on their surfaces (bottom, center, and top).

The electrical performance (R_E) of the systems was determined as a function of the net amount of electric power (P_E) generated per unit area of the panel (A_C), calculated as a function of the electrical parameters current (I_C) and voltage with load (V_C), according to [eq. (1)].

$$R_E = \frac{P_E}{A_C} = \frac{V_C \cdot I_C}{A_C} \quad (1)$$

Ten tests were carried out in total: five days for tests between PVT/w systems with a pump and the PV (PVT/w_CB X PV) and five days for tests between PVT/w systems without a pump and the PV (PVT/w_SB X PV). Among them, three tests were discarded due to weather instability in the observation period. Therefore, three tests were used for PVT/w_CB X PV and four tests for PVT/w_SB X PV. Data collection was carried out from 9:30 am to 2:00 pm, with measurements at thirty-minute intervals, totaling ten daily repetitions for each system and analyzed parameters.

The experimental design was completely randomized. The considered treatment groups were:

- System: referring to the PVT/w_CB X PV and PVT/w_SB X PV systems.
- Time: referring to the time of measurements, divided into ten 30-minute intervals.
- System X time: referring to the interaction between the type of system and the analyzed time to compare the behavior of the characteristic curve of each system at the analyzed interval.

The parameters average temperature of the panels, open-circuit voltage, voltage with load, electric current, and electric power were subjected to analysis of variance by the F-test to test the hypothesis that the variances of treatments are equal. Tukey's test was applied to compare the means when they were significant in the minimum order of 5% probability. The hourly comparison of results was performed quantitatively using linear and quadratic regression models.

RESULTS AND DISCUSSION

Weather data

Tables 1 and 2 show the main data obtained by the weather station during the set of measurements of the PVT/w_CB X PV and PVT/w_SB X PV systems, respectively.

The systems operated under similar average weather

conditions, with the PVT/w_CB X PV tests showing higher average ambient temperature values, in addition to a higher average wind speed. The recorded average global radiation values corroborated the historical means found using the models proposed by Oliveira et al. (2019) for the region of Mato Grosso do Sul, with the PVT/w_SB X PV tests standing out for being superior and more stable.

TABLE 1. Weather data from tests with PVT/w_CB X PV systems.

Day	Tmean (°C)	TM (°C)	Tm (°C)	U2 (m s ⁻¹)	Rs (kWh m ⁻² day ⁻¹)
June 23	21.3	28.2	14.5	0.73	3.92
July 2	12.1	27.1	-2.3	0.25	4.50
July 12	18.1	31.2	5.7	0.37	4.42
Mean	17.2	28.8	6.0	0.45	4.28

Tmean – Average ambient temperature, TM – Maximum ambient temperature, Tm – Minimum ambient temperature, U2 – Wind speed at 2 m above ground, Rs – Global radiation.

TABLE 2. Weather data from tests with PVT/w_SB X PV systems.

Day	Tmean (°C)	TM (°C)	Tm (°C)	U2 (m s ⁻¹)	Rs (kWh m ⁻² day ⁻¹)
July 5	15.4	28.8	3.6	0.20	4.28
July 7	16.1	27.2	4.5	0.33	4.25
July 9	16.4	28.2	4.4	0.30	4.56
July 13	19.3	32.2	6.4	0.35	4.50
Mean	16.8	29.1	4.7	0.30	4.40

Tmean – Average ambient temperature, TM – Maximum ambient temperature, Tm – Minimum ambient temperature, U2 – Wind speed at 2 m above ground, Rs – Global radiation.

Panel temperature

Figure 5 shows the panel temperature behavior of the PVT/w_CB X PV tests. The curves fitted by the quadratic regression model show that the highest values were reached around 12:37 pm by the PVT/w_CB system and around 12:44 pm by the PV system. Despite different ranges, the fitted curves showed a behavior statistically equal to each other (non-significant interaction), with the panel temperature being influenced by the type of system and time. The PV system had an average temperature of 48.20 °C

and the PVT/w_CB system of 54.34 °C (about 12.7% higher).

In contrast, Figure 6 shows the panel temperature behavior of the PVT/w_SB X PV tests. The curves fitted by the quadratic regression model show that the highest values were reached around 12:37 pm by the PVT/w_SB system and around 12:46 pm by the PV system. The fitted curves also showed a behavior statistically equal to each other (non-significant interaction), with the panel temperature being influenced by the type of system and time. The PV system had an average temperature of 51.28 °C and the PVT/w_CB system reached 58.87 °C (about 14.8% higher).

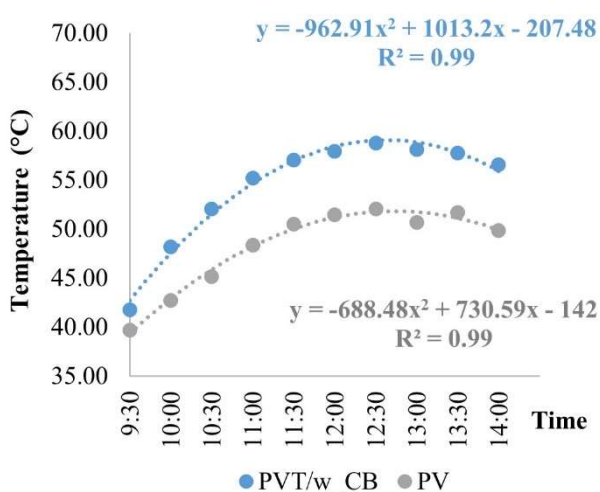


FIGURE 5. Average temperature values of the panels for PVT/w_CB X PV tests.

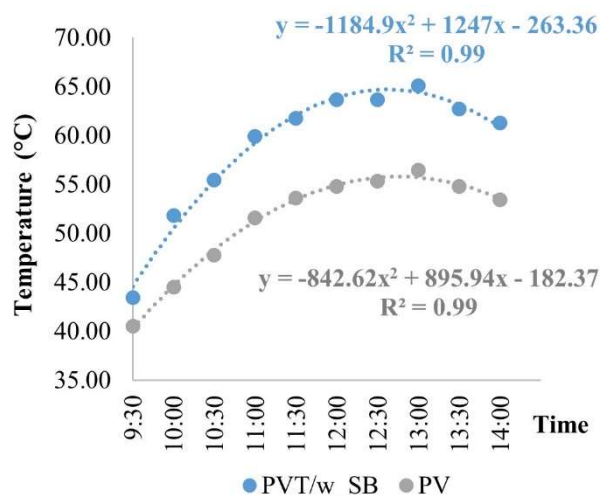


FIGURE 6. Average temperature values of the panels for the PVT/w_SB X PV tests.

The highest temperature values recorded for the PVT/w system in both tests demonstrate that the insulation at the rear helped to accumulate more heat in the system by decreasing the heat transfer with the medium, as observed by Dupré et al. (2017). On the other hand, it demonstrates that this heat accumulation was not sufficiently utilized by the adapted heat exchanger even with the use of the pump, leading to an increase in the panel temperature. For this reason, PVT/w systems reached their peak temperature earlier than PV systems and with higher intensity.

The comparison between PVT/w and PV systems in their respective tests demonstrates that the PVT/w_SB system had the highest average temperatures, being almost 15% higher than the PV system in its set of measurements (PVT/w_SB X PV).

Senthilraja et al. (2020) obtained maximum temperature values of 73 °C for a PV system and 58 °C for a PVT/w system at 12:00 pm, operating at a wind speed of

0.75 m s⁻¹, an ambient temperature of 38 °C, and global radiation of 950 W m⁻².

Open-circuit voltage

Figure 7 shows the behavior of the open-circuit voltage referring to the PVT/w_CB X PV tests. The PV system data were fitted to a linear regression model, while the PVT/w_CB system presented a quadratic fit. The fitted curves showed a behavior statistically different from each other (significant interaction), with the panel temperature being influenced by the type of system and time.

Figure 8 shows the behavior of the open-circuit voltage of the PVT/w_SB X PV tests. Both the PVT/w_SB system and the PV system were fitted by the quadratic regression model. These fitted curves also presented a behavior statistically different from each other (significant interaction), with the panel temperature being influenced by the type of system and time.

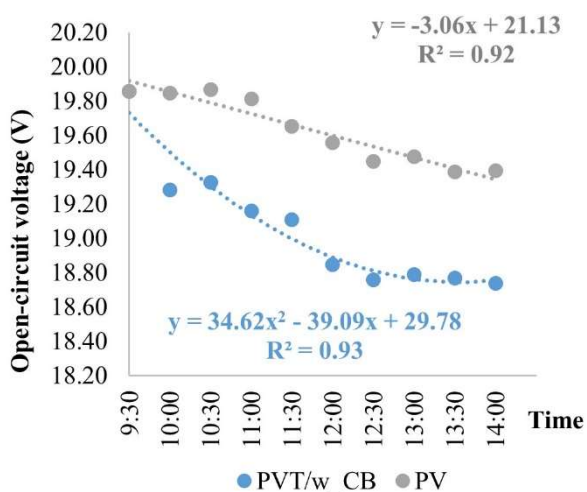


FIGURE 7. Average values of open-circuit voltage for PVT/w_CB X PV tests.

The open-circuit voltage has an inversely proportional relationship to the temperature and this relationship is referenced by the β coefficient on the panels (Maka & O'Donovan, 2022). It justifies the fact that the systems have presented characteristic curves different from each other, especially in the systems with higher temperatures, that is, the PVT/w systems, which were more affected by the temperature than the PV system. The initial measurements showed statistically equal values, as the equipment was at the same temperature, as observed by Jordan et al. (2021).

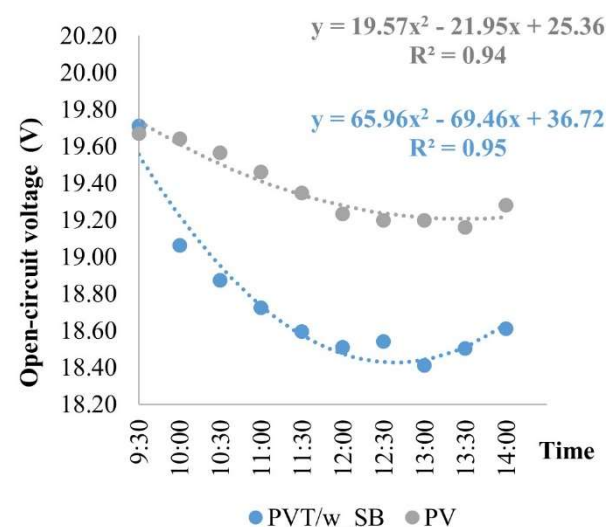


FIGURE 8. Average values of open-circuit voltage for PVT/w_SB X PV tests.

Voltage with load

Figure 9 shows the behavior of the voltage with load for the PVT/w_CB X PV tests. The curves fitted by the quadratic regression model show that the highest values were reached around 11:24 am by the PVT/w_CB system and around 11:50 am by the PV system. Despite different ranges, the fitted curves showed a behavior statistically equal to each other (non-significant interaction), with the voltage with load influenced by the type of system and time. The PV system had an average voltage with load of 16.43 V, while the PVT/w_CB system had an average voltage with load of 15.96 V (about 2.9% lower).

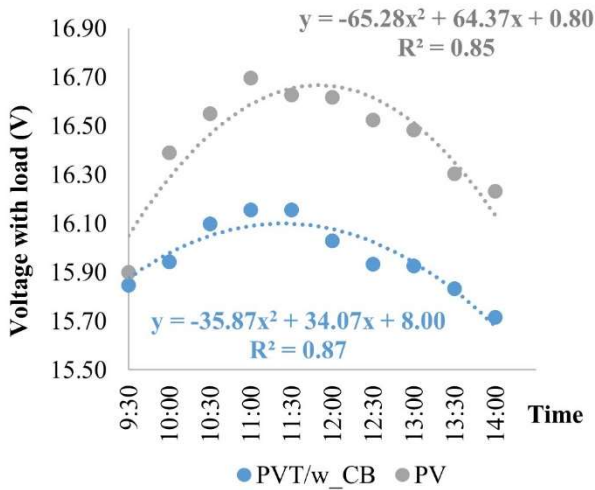


FIGURE 9. Average values of voltage with load for PVT/w_CB X PV tests.

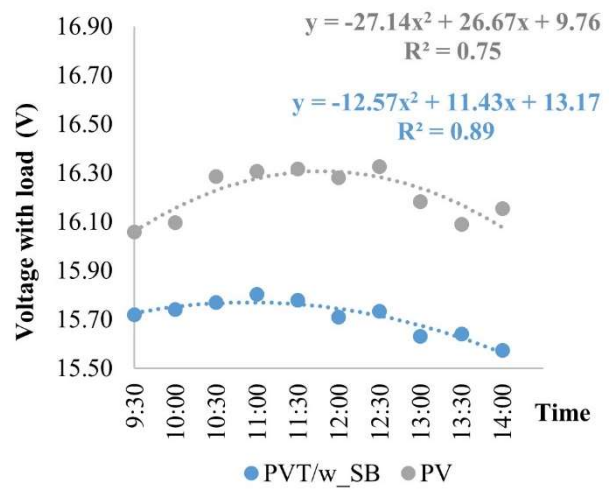


FIGURE 10. Average values of voltage with load for PVT/w_SB X PV tests.

Figure 10 shows the behavior of the voltage with load for the PVT/w_SB X PV tests. The curves also fitted by the quadratic regression model showed that the highest voltage values were reached around 10:55 am by the PVT/w_SB system and around 11:47 am by the PV system. The fitted curves also showed a behavior statistically equal to each other (non-significant interaction) and the voltage with load was also influenced by the type of system and time. The PV system presented an average voltage with load of 16.21 V, while the PVT/w_SB system presented an average value of 15.71 V (about 3.2% lower).

According to Liang et al. (2022), the voltage with load tends to be proportional to the incident radiation, which justifies the similar behavior of the voltage values to the radiation curves. The fact that the PVT/w systems presented lower values of voltage with load than the PV system in the tests together demonstrates that the cell temperature significantly influenced the output values, as observed by Khodadadi & Sheikholeslami (2022). For this reason, the PVT/w_SB system, with the highest temperature among the systems, presented the lowest values of voltage with load, reaching its peak value before the other systems (10:55 am against 11:24 am for the PVT/w_CB).

Electric current

Figure 11 shows the behavior of the electric current for the PVT/w_CB X PV tests. The curves fitted by the quadratic regression model show that the highest average values were reached around 11:13 am by the PVT/w_CB system and around 11:53 am by the PV system. Despite different ranges, the fitted curves showed a behavior statistically equal to each other (non-significant interaction), with the electric current being influenced by the type of system and time. The PV system presented an average value of electric current equal to 4.75 A and the PVT/w_CB system had an average value equal to 4.64 A (about 2.4% lower).

In contrast, Figure 12 shows the behavior of the electric current for the PVT/w_SB X PV tests. The curves also fitted by the quadratic regression model show that the highest average values were reached around 11:26 am by the PVT/w_SB system and around 11:50 am by the PV system. The fitted curves also showed a behavior statistically equal to each other (non-significant interaction) and the electric current was also influenced by the type of system and time. The PV system had an average value of electric current equal to 4.68 A, while the PVT/w_SB system had an average value of 4.55 A (about 2.9% lower).

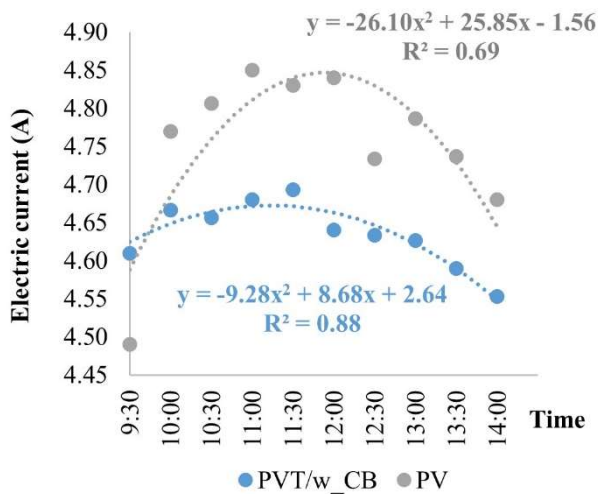


FIGURE 11. Average current values for PVT/w_CB X PV tests.

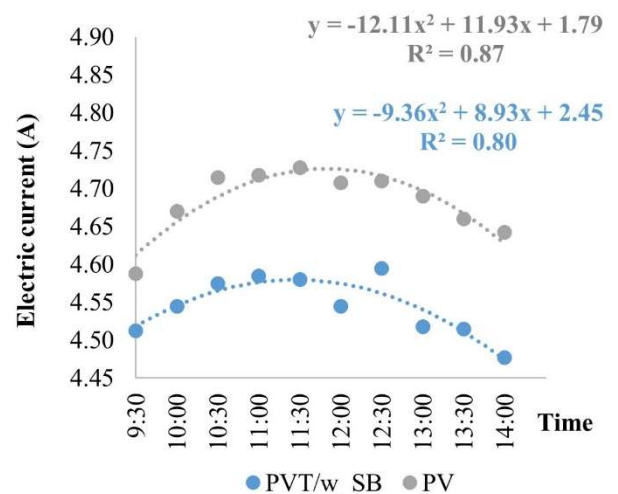


FIGURE 12. Average current values for PVT/w_SB X PV tests.

Similar to the voltage with load, the electric current was also directly influenced by the incident solar radiation and discretely by the temperature, as it affects the electrical properties of semiconductors and other components of the cell (Verduci et al., 2022).

Electric power

Figure 13 shows the electric power behavior for the PVT/w_CB X PV tests. The curves fitted by the quadratic regression model show that the highest average values were reached around 11:19 am by the PVT/w_CB system and around 11:51 am by the PV system. Despite different ranges, the fitted curves showed a behavior statistically equal to each other (non-significant interaction), with the

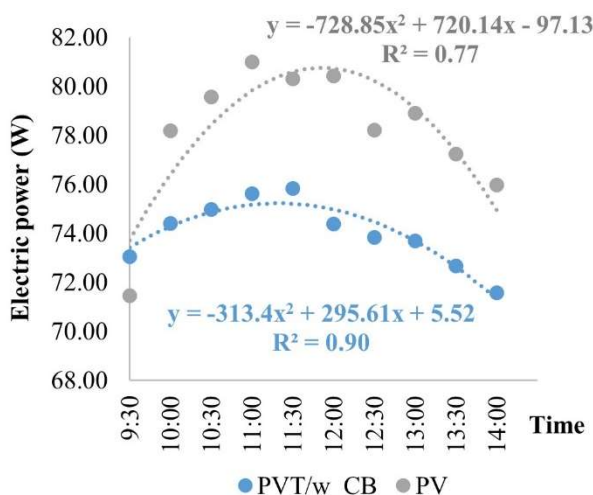


FIGURE 13. Average values of electric power for PVT/w_CB X PV tests.

The electric power of panels is determined as a function of the generated voltage and electric current and, for this reason, its behavior follows the same pattern of these magnitudes, with a direct relationship with solar radiation and an inversely proportional relationship with temperature, referenced by the coefficient of performance γ (Piotrowski & Farret, 2022). Therefore, the PV system presented the highest

TABLE 3. Electrical performance for PVT/w_CB X PV tests.

Measurement	PVT/w_CB		PV	
	Average panel temperature (°C)	Electrical performance (W m ⁻²)	Average panel temperature (°C)	Electrical performance (W m ⁻²)
June 23	52.08	74.27	45.85	78.53
July 2	53.13	75.47	47.11	79.77
July 12	57.79	72.29	51.63	76.10
Mean	54.34	74.01	48.20	78.13

TABLE 4. Electrical performance for PVT/w_SB X PV tests.

Measurement	PVT/w_SB		PV	
	Average panel temperature (°C)	Electrical performance (W m ⁻²)	Average panel temperature (°C)	Electrical performance (W m ⁻²)
July 5	55.77	71.68	48.86	75.70
July 7	58.65	71.57	50.35	75.99
July 9	60.15	71.17	52.32	75.91
July 13	60.89	71.18	53.59	76.03
Mean	58.87	71.40	51.28	75.91

electric power being influenced by the type of system and time. The PV system had an average value of 78.13 W, while the PVT/w_CB system had an average value of 74.01 W (about 5.6% lower).

On the other hand, Figure 14 shows the electric power behavior for the PVT/w_SB X PV tests. The curves also fitted by the quadratic regression model show that the highest average values were reached around 11:18 am by the PVT/w_SB and around 11:49 am by the PV system. The fitted curves also showed a behavior statistically equal to each other (non-significant interaction) and the electric power was also influenced by the type of system and time. The PV system presented an average of 75.91 W and the PVT/w_SB system had an average of 71.40 W (6.3% lower).

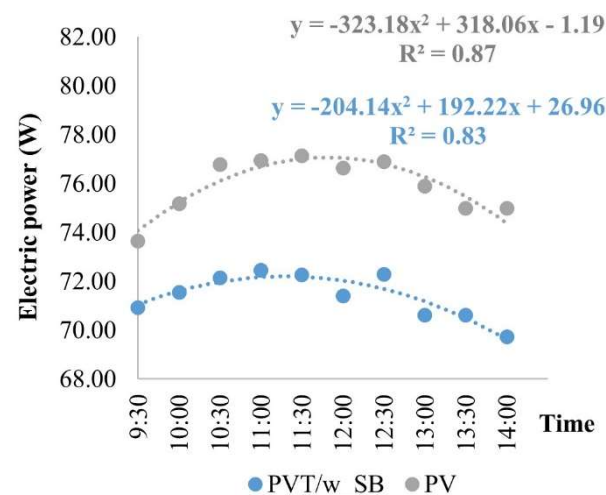


FIGURE 14. Average values of electric power for PVT/w_SB X PV tests.

electric power values compared to the PVT/w systems in their respective tests, as it worked with the lowest temperatures.

Electrical performance

Tables 3 and 4 show the electrical performance of the PVT/w_CB X PV and PVT/w_SB X PV systems.

The average panel temperature presented a negative effect on the electrical performance of the systems. The PV system presented the lowest temperature values in both tests and, consequently, had the highest electrical performance values, followed by the PVT/w_CB and PVT/w_SB systems. The best results for the PV system were obtained during the PVT/w_CB X PV test set, with an average electrical performance of 78.13 W m^{-2} , as these measurements were carried out in a period with lower maximum temperatures and higher wind speeds (Tables 2 and 3), which are also parameters that influence the electrical performance of the panel (Abdullah et al., 2019). The PVT/w_CB and PVT/w_SB systems showed average electrical performances of 74.01 and 71.40 W m^{-2} , respectively.

In both cases, the electrical performance of the PVT/w systems was slightly lower than their respective PV systems, as it was a closed system (thermos-accumulative): the temperature in the reservoir will be higher every hour, causing the values of inlet and outlet temperatures of water in the panel to also be higher, reducing the amount of heat absorbed by the heat exchanger. This heat accumulation of increases the temperature of the panel and reduces its electrical performance.

The actual potential of the proposed system must be evaluated considering the global performance, that is, the electrical and thermal performance. According to Sathe & Dhoble (2017), PVT/w systems have good applicability in ambient air conditioning, water heating systems (domestic and industrial), water distillation, and food processing.

As a reference, Medeiros et al. (2021) developed a study with a PVT/w system, in which the photovoltaic panel had its rear completely closed by an acrylic plate, without insulation, with cooling water in direct contact with the photovoltaic cell, via forced circulation by gravity (average flow of 20 L/h), and without recirculation, and obtained an average electrical performance of 101.12 W m^{-2} in a photovoltaic panel whose maximum theoretical electrical performance was 108 W m^{-2} .

Jordan et al. (2021) found an average electrical performance of 117 W m^{-2} in a photovoltaic panel whose maximum theoretical electrical performance was 136 W m^{-2} . The system consisted of a photovoltaic panel with the rear closed by iron plates and plywood, where the panel frame was also used as a channel with the cooling water in direct contact with the photovoltaic cell via forced circulation.

Kim & Kim (2012) obtained an average electrical performance of 126 W m^{-2} for a shell-and-tube system in a photovoltaic panel whose maximum theoretical electrical efficiency was 145 W m^{-2} .

CONCLUSIONS

This study aimed to analyze the electrical performance of a PVT/w system with natural and forced circulation. Among the PVT/w systems, the highest electrical performance was obtained by the PVT/w_CB system, but both showed an increase in the temperature of the photovoltaic cell when compared to the PV system, indicating great thermal potential and influence of the flow rate. Thus, the actual potential of the systems can only be determined also considering the use of the obtained thermal portion.

The PV system presented different values of electrical performance in each set of measurements, with the best results during the PVT/w_CB X PV studies, which experienced more expressive winds and lower maximum temperatures.

The temperature of the photovoltaic cell influenced the electrical parameters, with a trend to decrease as the temperature increased, as observed in the voltage with load, electric current, electric power, and, consequently, the electrical performance.

The use of a bank of fixed load resistors presented a simple and practical way of analyzing the electrical performance of systems in general.

REFERENCES

- Abdullah AL, Misha S, Tamaldin, N, Rosli MAM, Sachit FA (2019) A review: parameters affecting the PVT collector performance on the thermal, electrical, and overall efficiency of PVT system. *Journal of Advanced Research in Fluid Mechanics and Thermal Sciences* 60(2):191–232. Available: <https://akademibaru.com/submit/index.php/arfmts/article/view/2643/1707>. Accessed: Jul 19, 2022.
- Ahmed OK, Hamada KI, Salih AM (2019) Performance analysis of PV/Trombe with water and air heating system: an experimental and theoretical study. *Energy Sources, Part A: Recovery, Utilization, and Environmental Effects* 44(1):2535-2555. DOI: <https://doi.org/10.1080/15567036.2019.1650139>.
- Alvares CA, Stape JL, Sentelhas PC, Gonçalves JLM, Sparovek G (2013) Köppen's climate classification map for Brazil. *Meteorologische Zeitschrift* 22(6):711-728. DOI: <https://doi.org/10.1127/0941-2948/2013/0507>.
- Cotfas DT, Cotfas PA, Mahmoudinezhad S, Louzazni M (2022) Critical factors and parameters for hybrid Photovoltaic-Thermoelectric systems; review. *Applied Thermal Engineering* 215:118977. DOI: <https://doi.org/10.1016/j.applthermaleng.2022.118977>.
- Dupré O, Vaillon R, Green MA (2017) *Thermal behavior of photovoltaic devices: physics and engineering*. Springer, 220 p. DOI: <https://doi.org/10.1007/978-3-319-49457-9>.
- Hajjaj C, Benhmida M, Bendaoud R, Amiry H, Bounour S, Ghennioui A, Chanaa F, Yadir S, Elhassnaoui A, Ezzaki H (2019) A PVT cooling system design and realization: temperature effect on the PV module performance under real operating conditions. *International Journal of Renewable Energy Research* 9(1). DOI: <https://doi.org/10.20508/ijrer.v9i1.8789.g7598>.
- Hassan A, Wahab A, Qasim MA, Janjua MM, Ali MA, Ali HM, Jadoon TR, Ali E, Raza A, JAVAID N (2020) Thermal management and uniform temperature regulation of photovoltaic modules using hybrid phase change materials-nanofluids system. *Renewable Energy* 145:282-293. DOI: <https://doi.org/10.1016/j.renene.2019.05.130>.
- Hossain MS, Pandey AK, Selvaraj J, Rahim NA, Rivai A, Tyagi VV (2019) Thermal performance analysis of parallel serpentine flow based photovoltaic/thermal (PV/T) system under composite climate of Malaysia. *Applied Thermal Engineering* 153:861-871. DOI: <https://doi.org/10.1016/j.applthermaleng.2019.01.007>.

- Jordan RA, Moreira Junior O, Antunes BM, Motomiya AVA, Sanches IS, Sanches ES, Omido AR, Martins EAS (2021) Desempenho de um painel fotovoltaico (PV) convertido em um fotovoltaico térmico com coletor para água quente (PVT/w). *Research, Society and Development* 10:(7):e14210716438. DOI: <https://doi.org/10.33448/rsd-v10i7.16438>.
- Khodadadi M, Sheikholeslami M (2022) Review on poly-generation application of photovoltaic/thermal systems, *Sustainable Energy Technologies and Assessments* 52:102172. DOI: <https://doi.org/10.1016/j.seta.2022.102172>.
- Kern Jr EC, Russel MC (1978) Combined photovoltaic and thermal hybrid collector systems. *Proceedings of the 13th ISES Photovoltaic Specialists*. Washington, Proceedings... DOI: <https://doi.org/10.2172/7151726>.
- Lammle M, Kramer K, Hermann M (2017) Assessing suitable fields of application for PVT collectors with the characteristic temperature approach. Freiburg, Fraunhofer Institute for Solar Energy Systems ISE. DOI: <https://doi.org/10.18086/swc.2017.18.10>.
- Liang S, Zheng H, Wang X, Ma X, Zhao Z (2022) Design and performance validation on a solar louver with concentrating-photovoltaic-thermal modules. *Renewable Energy* 191:71-83. DOI: <https://doi.org/10.1016/j.renene.2022.04.041>.
- Maka AO, O'Donovan TS (2022) Effect of thermal load on performance parameters of solar concentrating photovoltaic: high-efficiency solar cells. *Energy and Built Environment* 3:201-209. DOI: <https://doi.org/10.1016/j.enbenv.2021.01.004>.
- Medeiros RRB, Lima AVNA, Diniz GF, Melo VM, De Souza LGM, Da Silva KCG (2021) Estudo de desempenho de um sistema híbrido fotovoltaico/térmico. *Research, Society and Development* 10(7): e1210716156. DOI: <http://dx.doi.org/10.33448/rsd-v10i7.16156>
- Oliveira SS, Cavazzana GH, Souza A (2019) Estimativa da radiação solar global em função da temperatura do ar e isolinhas para o Estado de Mato Grosso do Sul, Brasil. *Revista Brasileira de Gestão Ambiental e Sustentabilidade* 6(12):93-108. DOI: <http://dx.doi.org/10.21438/rbgas.061207>
- Ouédraogo A, Zouma B, Ouédraogo E, Guissou L, Bathiébo DJ (2021) Individual efficiencies of a polycrystalline silicon PV cell versus temperature, *Results in Optics* 4:100101. DOI: <https://doi.org/10.1016/j.rio.2021.100101>.
- Piotrowski LJ, Farret FA (2022) Feasibility of solar tracking and fixed topologies considering the estimated degradation and performance of photovoltaic panels. *Solar Energy Materials and Solar Cells* 244:111834. DOI: <https://doi.org/10.1016/j.solmat.2022.111834>.
- Queiroz AO, Brito AU (2020) Direct connection photovoltaic system in multi-motor application for the rural sector. *Engenharia Agrícola* 40(3):303-314. DOI: <https://doi.org/10.1590/1809-4430-Eng.Agric.v40n3p303-314/2020>.
- Rahman A, Farrok O, Haque MM (2022) Environmental impact of renewable energy source based electrical power plants: Solar, wind, hydroelectric, biomass, geothermal, tidal, ocean, and osmotic, *Renewable and Sustainable Energy Reviews* 161:112279, DOI: <https://doi.org/10.1016/j.rser.2022.112279>.
- Sathe TM, Dhoble AS (2017) A review on recent advancements in photovoltaic thermal techniques. *Renewable and Sustainable Energy Reviews* 76:645-672. DOI: <https://doi.org/10.1016/j.rser.2017.03.075>.
- Senthilraja S, Gangadevi R, Marimuthu R, Baskaran M (2020) Performance evaluation of water and air based PVT solar collector for hydrogen production application. *International journal of hydrogen energy* 45(13):7498-7507. DOI: <https://doi.org/10.1016/j.ijhydene.2019.02.223>.
- Tarbi A, Chtouki T, Bouich A, Elkouari Y, Erguig H, Migalska-Zalas A, Aissat A (2022) InP/InGaAsP thin films based solar cells: Lattice mismatch impact on efficiency. *Optical Materials* 131:112704. DOI: <https://doi.org/10.1016/j.optmat.2022.112704>.
- Tiwari S, Agrawal S, Tiwari GN (2018) PVT air collector integrated greenhouse dryers. *Renewable and Sustainable Energy Reviews* 90:142-159. DOI: <https://doi.org/10.1016/j.rser.2018.03.043>.
- UN - United Nations (2022) World population prospects. Department of Economic and Social Affairs: Population Division. Available: <https://population.un.org/wpp/>. Accessed Jul 19, 2022.
- Verduci R, Romano V, Brunetti G, Nia NY, Di Carlo A, D'Angelo G, Ciminelli C (2022) Solar energy in space applications: review and technology perspectives. *Advanced Energy Materials* 12(29):2200125. DOI: <https://doi.org/10.1002/aenm.202200125>.